ARCHIVES OF MECHANICS
Arch. Mech. **75** (6), 647–672, 2023, DOI: 10.24423/aom.4359

Grain refinement, microhardness distribution, strain hardening behaviour and mechanical proprieties of RD-ECAPed AA 1050

A. HALIMI*), L. HEMMOUCHE, I. E. CHETTAH, Z. A. LOUCHENE

Laboratoire Génie des Matériaux, École Militaire Polytechnique,
BP17 Bordj El-Bahri, 16046 Algiers, Algeria, ORCID: 0000-0001-7439-9032,
e-mail): halimi.amel.18@gmail.com (corresponding author)*

This study aims to investigate the evolution of mechanical and microstructural characteristics of the 1050 aluminium alloy processed by Rotary Die Equal Channel Angular Pressing (RD-ECAP). The RD-ECAPed specimens were analysed after each pass using optical microscopy, quasi-static compression test and microhardness measurements. The results revealed a reduction in grain size from 29 μm before the RD-ECAP process to a minimum value of 2 μm at the second pass, corresponding to the maximum value of compressive yield strength, reaching 184 MPa. Furthermore, there was an increase in hardness from 30 Hv to 63 Hv with a homogeneous distribution along the longitudinal surface, especially in the initial four RD-ECAP passes. Additionally, the appearance of a 45° shear plane was observed at the last fifth pass, coinciding with the region of maximum microhardness.

Key words: aluminium alloys, Rotary Die Equal Channel Angular Pressing, microstructure, longitudinal microhardness, compression test.

1. Introduction

The development of advanced materials that meet ever-increasing requirements is a primary goal of materials science. The refinement of grain size is one of the approaches used to enhance the mechanical properties of materials through the standard Hall–Petch relationship [1, 2], which described the influence of the grain size on the hardness and strength of polycrystalline material. As the grain size decreases, both its hardness and strength increase. Various techniques can be employed to achieve refinement of grain size in materials; including severe plastic deformation (SPD) methods [3, 4]. Sheik Hassan *et al.* [5] highlighted the development of different SPD methods and the production of diverse materials with improved results tailored to specific requirements. Valiev *et al.* [6] and Valiev [7] give particular attention to the new concepts and principles of using various severe plastic deformation (SPD) processing methods for producing bulk nanostructured metals, emphasizing the correlation between microstructural features and properties. Besides, Wang *et al.* [8] discussed the

significant interest in ultrafine-grained materials achieved through severe plastic deformation (SPD) techniques. The focus is on introducing SPD methods, with particular attention given to two novel techniques, Elliptical Cross-section Spiral Channel Extrusion with Equal-area (ECSEE) and Elliptical Cross-section Spiral Channel Drawing with Equal-area (ECSDE). Moreover, the Accumulative Roll Bonding (ARB) process is considered one of the most effective Severe Plastic Deformation techniques for producing Ultrafine-Grained materials. It was introduced by Saito in 1998 [9]. In our previous work [10], we investigated the quasi-static and dynamic characterization of 2017A-T4 aluminium alloy processed by accumulative roll bonding. The conditions of the ARB process, along with the composition and microstructure of the base material, play an important role in the mechanical behaviour and the microstructure evolution of the ARBed alloy. Sahoo *et al.* [11] studied the microstructure and hardness of Ti-6Al-4V alloy sheets processed by asymmetrical cryorolling, warm rolling, and hot rolling with up to 75% thickness reductions, leading to ultrafine grain refinement. Cryorolling exhibits the lowest grain sizes resulting in the highest hardness, and the phase analysis of the dual-phase Ti-($\alpha + \beta$) alloy revealed the influence of β-Ti phase, providing insights into mechanical properties.

Furthermore, the high-pressure torsion (HPT) is indeed a well-recognized Severe Plastic Deformation technique, widely used to achieve significant grain refinement and enhance the mechanical properties of materials. Specifically, HPT applies both compressive force and torsional straining to the material [12, 17]. Zhilyaev *et al.* [13] selected pure nickel for a detailed investigation of the experimental parameters influencing grain refinement and microstructural evolution during processing by high-pressure torsion. They proposed a simple model to explain the development of a homogeneous microstructure in the HPT process.

Otherwise, Equal Channel Angular Pressing (ECAP) is another Severe Plastic Deformation technique. It involves pressing a material through a channel with two intersecting channels, which promotes significant plastic deformation and grain refinement. ECAP is a well-established SPD process used to enhance the mechanical properties of materials by creating ultrafine-grained structures [14, 15]. Segal [16] was the first to apply the ECAE process, exploring stress, strain, shear planes, steady and localized flow, and multipass processing, emphasizing the role of these factors in defining microstructural effects crucial for the achieved results. Vishnu *et al.* [18] and Cui *et al.* [19] investigated the effects of processing metallic materials such as titanium alloys, aluminum alloys, and magnesium alloys using various process parameters in the Equal Channel Angular Pressing die. The study aimed to explore the advancements, challenges, and outcomes associated with the application of ECAP, focusing on the evolution of grain sizes, grain boundaries, and phases of different metallic materials,

alongside the plastic deformation mechanism during the ECAP process. SAHOO *et al.* [20] investigated the mechanical and microstructural characteristics of the Ti-6Al-4V alloy processed by ECAP, leading to ultrafine grain refinement and a reduction in the β-phase, thereby improving room temperature hardness and tensile strength. HORITA *et al.* [21] explored severe plastic deformation as a way to introduce fine grain sizes into polycrystalline materials, interesting on the ECAP terms, and the microstructure evolution was influenced by factors such as the processing route, die channel angle, and pressing speed and temperature. Besides, the ECAP process can be performed using various routes by rotating the sample between passes, including the A, B, and C routes, resulting in shear in different planes [22]. The A route involves rotating the sample 180 degrees between each pass, while the B route involves rotating the sample by 90 degrees. The C route involves a combination of the A and B routes. Each route has a significant impact on the microstructure and properties of the material [23]. The choice of the ECAP route can have a great influence on the microstructure and mechanical properties of the material. However, different pathways can give rise to different grain sizes, textures, and dislocation densities, which in turn influences the mechanical behaviour of the material, such as strength, ductility, and toughness [24, 25]. KUMAR *et al.* [26] revealed the influence of the ECAP route on the microstructure and mechanical properties of aluminium alloy 7075, with the BC route showing superior strength and the C route exhibiting better elongation, and VENKATACHALAM *et al.* [27] demonstrated that the BC route was found to result in a refined equiaxed microstructure, superior mechanical properties, and smaller grain size of aluminium alloy 2014 compared to other routes which lead to the importance of selecting appropriate ECAP routes for achieving desired mechanical properties and provide valuable insights for optimizing the processing parameters of ECAP for alloy refinement.

Further, ECAP results in a refined microstructure, characterized by small, equiaxed grains with a high density of grain boundaries [28]. The grain size can be reduced to the nanoscale, which can result in improved mechanical properties, such as increased strength and ductility [29]. The strength of the material is typically increased due to the refinement of the grain structure, while the ductility is increased due to the high density of grain boundaries [30]. The ECAP process has several parameters that can be adjusted to control the deformation of the material, including the temperature, strain rate, number of passes, and the angles of the channel [31]. The temperature is typically chosen to be below the recrystallization temperature to prevent the formation of new grains during the process [32]. Various researches show that the ECAP process can effectively improve the microstructure and the mechanical proprieties, but the ECAPed material behaviour is influenced by the pressing temperature condi-

tions [33, 34]. At low temperatures (cryogenic temperature), dislocation sliding, dynamic recovery, and texture evolution was restrained, thereby resulting in materials with higher strength compared to room temperature [35]. That can be attributed to two main mechanisms: grain boundary strengthening and dislocation strengthening. However, the microstructure and bulk texture resulting from ECAP at low temperatures led to the increased grain boundary density and the reduced grain size, which in turn enhanced the grain boundary strengthening effect and contributed to the higher strength of the material. Moreover, the temperature modification during the ECAP process can have a significant impact on the microstructure and mechanical properties of Al-7075 alloy [36], which at lower temperatures may result in finer grains and better mechanical properties, while higher temperatures may lead to coarsening of grains and precipitates, resulting in decreased mechanical properties. Nevertheless, the post-processing ECAP at lower annealing temperatures can help to maintain the improved properties obtained from ECAP, while annealing at higher temperatures may lead to a decrease in hardness due to grain growth [37, 38].

The strain rate is also critical in controlling the deformation, and it can be adjusted by changing the speed of the press [39, 40]. Likewise, the number of passes is also a crucial parameter that can affect the final microstructure and mechanical properties of the material. The findings of Abioye *et al.* [41] study highlight the importance of the number of passes in the ECAP process in determining the mechanical behaviour of aluminium alloys. The initial passes may result in a significant increase in strength due to the presence of a high density of dislocations, but the effect may diminish as the saturation point of dislocation density is reached. Moreover, the directional dependence of stresses and strains decreased with increasing ECAP passes, leading to more isotropic behaviour in the material at the measured length scale [42]. Furthermore, designing the ECAP die geometry to achieve optimum strain distribution homogeneity is more suitable than optimizing the effective strain magnitude. It is important to note that the choice of die channel angles and outer corner angles significantly influenced the strain distribution behaviour in the ECAPed material [43, 44].

The aim of this study is to explore the impact of severe plastic deformation (SPD) on the mechanical and microstructural properties of the 1050 aluminium alloy using the Rotary Die Equal Channel Angular Pressing (RD-ECAP) technique. The RD-ECAP process involves applying a load to the sample using a hydraulic press through four perpendicular circular-shaped extrusion channels of a one-piece rotary die. The process is repeated for up to 10 passes at room temperature with optimized processing parameters and sample geometric. The microstructure evolution after severe deformation processing was examined to determine the progression of grain size. Moreover, the evolution of longitudinal microhardness trough the pressing direction was investigated at each RD-ECAP

pass. Besides, the mechanical proprieties and the strain hardening behaviour of the RD-ECAPed samples were studied in the context of the compression test in a function of the number of passes.

2. Experimental methods

Equal Channel Angular Pressing (ECAP) is a severe plastic deformation technique used to refine the grain structure of a material, leading to the development of ultrafine-grained (UFG) or nanostructured materials [16]. The principle is to press a sample, usually a bar of a metal, through a die composed of two channels of equal cross-sectional area meeting at an angle. The sample is pushed through the die repeatedly along different routes to induce plastic deformation without changing the overall shape of the sample. The internal angle between the channels of the die is typically between 90° and 135°. As the sample is pushed through the die, it undergoes large plastic strains in the area of the intersection of the channels. The sample is typically rotated between passes to ensure that each pass deforms the material in a different direction, resulting in significant grain refinement. The shear stress at the interior angle of the extrusion channel causes dislocations to pile up and form new grains with a smaller size, leading to the formation of UFG or nanostructured materials. The resulting material can have improved mechanical properties such as increased strength, ductility, and wear resistance.

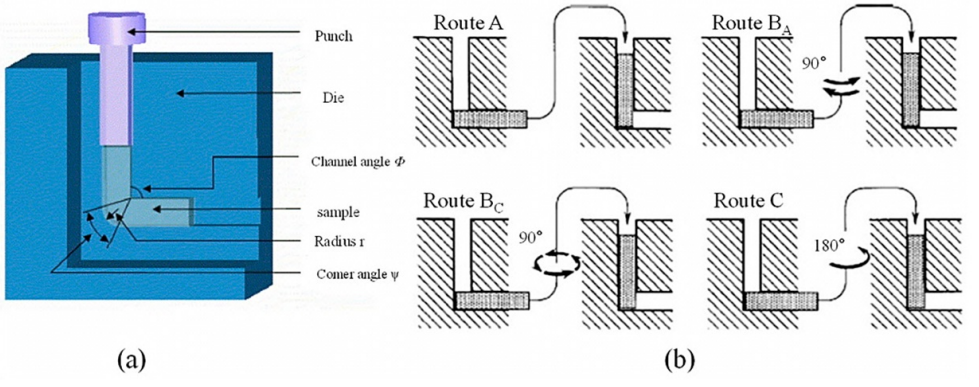

FIG. 1. (a) Schematic illustration of a typical ECAP. (b) Schematic diagram of different routes [19].

The piston speed, die temperature, and channel angles, can have a significant impact on the microstructure, texture, and defect density of ultrafine-grained (UFG) materials produced through the ECAP process. For instance, the piston speed can affect the strain rate and the level of deformation applied to the mate-

rial, which in turn can influence the grain size and the resulting microstructure. Similarly, the die temperature can affect the deformation behaviour of the material and its resulting microstructure, with higher temperatures often leading to coarser grains and a more equiaxed microstructure [33–36]. The channel angles used in the SPD process can also have an impact on the microstructure and texture of the UFG material, with different angles leading to different deformation paths and strain distributions [39, 44]. The resulting microstructure, texture, and defect density of the UFG material, in turn, have a significant impact on the mechanical properties of the material, such as its strength, ductility, and toughness. Therefore, optimizing the ECAP parameters to achieve the desired microstructure and mechanical properties is an important aspect of the UFG material design and processing [23, 30, 50].

The ECAP device used in this study is based on the RD-ECAP (Rotary-Die ECAP) model, which was developed by researchers from the National Institute of Advanced Industrial Science and Technology in Nagoya, Japan [45, 46]. The classic ECAP process has some limitations, such as limited strain homogeneity and high processing forces. The RD-ECAP process overcomes some of these limitations by using a rotating die that can provide more uniform strain distribution and lower processing forces [46]. In this process, the billet is fed into the rotating die, which has one or more channels, and is pressed through the channels by a stationary punch without sample removal. The rotating die allows for continuous deformation and a more uniform distribution of strain throughout the sample.

Figure 2 represents the configuration of the RD-ECAP device used in this study. The device consists of several components, including:

- Die holder: this is the main body of the device that holds the die and other components in place.
- Die: this is the component that contains the channels through which the sample is pressed. The die is designed to rotate during the process.

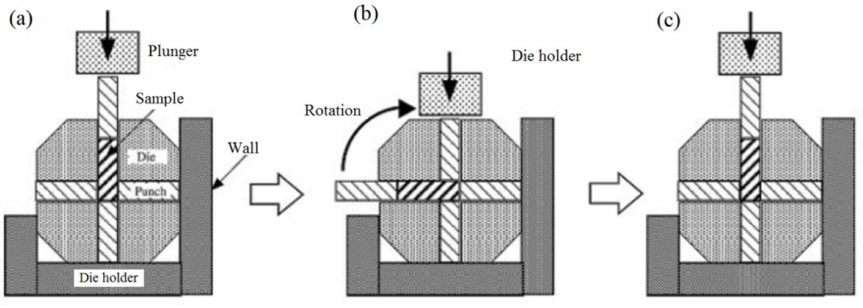

Fig. 2. Schematic illustration of the RD-ECAP process [45].

- Four punches: these are the components that apply the pressure to the sample as it is pressed through the die. The punches are arranged in a cross-like pattern around the die.
- Sample (Test piece): this is the bar of material that is being processed through the RD-ECAP device.
- Plunger: this component is used to apply pressure to the punches, which in turn apply pressure to the sample as it is pressed through the die.

The material used in this study is the AA1050 aluminium alloy. It is a pure aluminium alloy that contains no significant alloying elements and is therefore known for its high purity and good corrosion resistance. The AA1050 aluminium alloy specifically has a purity of more than 99.5% and is relatively homogeneous in composition. This alloy is commonly used in various industries, such as construction, welding ($T_f = 658°C$), boiler making ($Re = 53\,MPa$, $E = 69\,GPa$, $G = 25.9\,GPa$, $\nu = 0.33$), and packaging, due to its lightweight ($\rho = 2700\,kg \cdot m^{-3}$), good corrosion resistance, and suitability for surface treatments. The chemical composition of the 1050 aluminium alloy, acquired using the X-ray Fluorescence Spectrometer (EDX-800HS), is presented in Table 1.

TABLE 1. Chemical composition of the AA1050 aluminium alloy.

Elements	Fe	Si	Zn	Ti	Mg	Mn	Cu	Al
Composition [Wt. %]	0.4	0.25	0.07	0.05	0.05	0.05	0.05	Balance

The RD-ECAP device used in this study consists of a die holder, a die with 4 perpendicular channels then forming 2 active channels and 2 other inactive channels, in addition to 3 punches, including two blocking punches and a working punch. The sample is pressed through the die using a hydraulic press with a 100 ton capacity.

The die holder is an important component of the RD-ECAP device used to fix the die and prevent any movements during the extrusion process. In addition to holding the die in place, the die holder also helps to reinforce the blocking punches. The blocking punches are used to prevent material from flowing into the inactive channels of the die during extrusion. By applying compression using the hydraulic press, the blocking punches are strengthened, ensuring that they can effectively block the inactive channels and force the material through the active channel of the die.

During the RD-ECAP process the lubrication (with grease) was using to reduce friction and wear between the sample and the die, which can cause damage to the device and affect the quality of the processed material. Lubrication also helps in reducing the required pressing force, improving the material flow, and enhancing the homogeneity of the processed material. The grease chosen in this study is a semisolid lubricant consisting of oil and a thickening agent, is com-

monly used for high-temperature and high-load applications because of its ability to adhere to the surfaces, resist water and prevent metal-to-metal contact. Its high viscosity ensures that it stays in place and provides a barrier against wear and tear.

The installation of our RD-ECAP device shown in Fig. 3 involves the following steps:

- Place the blocking punches in the inactive channels (lower and rear) of the device.
- Lubricate the sample and insert it into the upper active channel of the device.
- Place the assembly (die and punches) in the die holder of the device.
- Insert the work punch between the plunger of the hydraulic press and the sample.
- Extrusion process is then operated.
- Rotation of the die without removing the sample and continue the next pressing up to 10 passages.

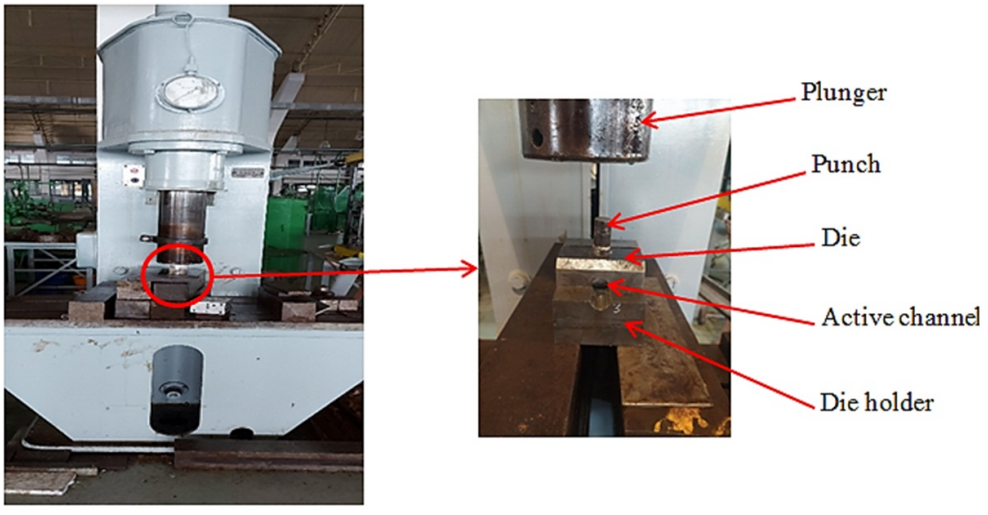

Fig. 3. Experimental installation of RD-ECAP process.

To succeed in the RD-ECAP process, a numerical simulation has been carried out on the design of the ECAP device and the choice of operating conditions (channel angles, pressing speed, route, and temperature) and the sample size and geometry (diameters, lengths, and shape) to find the optimal combination of parameters that produced the desired material properties. The operating conditions used in this study were summarized in Table 2.

TABLE 2. Processing parameters of RD-ECAP process.

Temperature [°C]	25
Pressing speed [mm/s]	2
Route	A
Internal angle ϕ [°]	90
External angle ψ [°]	0
Sample diameters [mm]	19.5
Sample lengths [mm]	40
Sample shape	Truncated cylinder

The RD-ECAP process was successful in producing high-quality samples of AA1050 aluminium alloy after ten passes without developing any defects (Fig. 4). This means that the process was executed correctly and that the material was able to withstand the applied deformation without any failure such as porosity, shear cracking, buckling, etc.

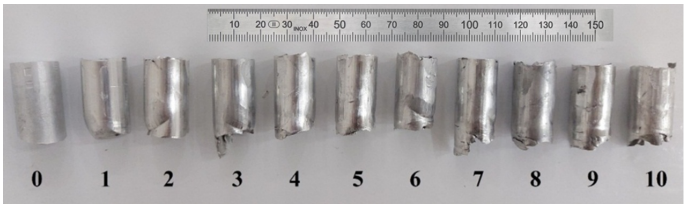

FIG. 4. Samples obtained after each RD-ECAP pass.

The absence of defects in the processed samples suggests that the RD-ECAP process was able to achieve a uniform distribution of the deformation across the material, which is essential for avoiding stress concentrations that can lead to the formation of defects. This indicates that the resulting material is likely to have a more homogeneous microstructure, which can translate into improved mechanical properties such as increased strength, ductility, and fatigue resistance.

The evolution of the equivalent effective plastic strain with the number of RD-ECAP passes is an important parameter to monitor during the elaboration of a UFG material. It is a measure of the total amount of plastic strain that a material has undergone during processing, which is related to the degree of the microstructure refinement.

In the current study, the equivalent effective plastic strain ($\varepsilon_{\mathrm{eq}}$) is determined after each ECAP pass using the specified mathematical expression bellow, where N corresponds to the number of ECAP passes, while ϕ and ψ represent the internal and external angles of the ECAP channel, respectively. For our specific

case study, the parameters are defined as follows: N ranges from 0 to 10, with ϕ set at 90° and ψ at 0°

$$\varepsilon_{\text{eq}} = \left(\frac{N}{\sqrt{3}}\right)\left[2\cot\left(\frac{\phi}{2}+\frac{\psi}{2}\right)+\psi\csc\left(\frac{\phi}{2}+\frac{\psi}{2}\right)\right] \quad [43].$$

The equivalent plastic strain, presented in Fig. 5, increases linearly with the number of ECAP passes, which is consistent with the behaviour typically observed during ECAP processing. As more passes are applied, the material is subjected to a greater amount of plastic deformation, which can lead to a more refined microstructure and improved mechanical properties.

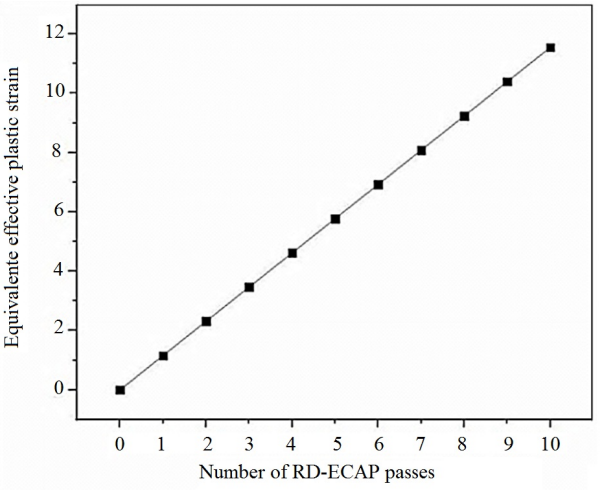

Fig. 5. Evolution of the equivalent effective plastic strain as a function of the number of ECAP passes.

However, the relationship between the equivalent plastic strain and the resulting microstructure can be complex and depends on several factors such as the initial microstructure, processing parameters, and the properties of the material. In some cases, an excessive amount of plastic deformation can lead to the formation of defects, such as cracking or voids, which can degrade the mechanical properties of the material [3]. Therefore, it is important to carefully monitor the evolution of the equivalent plastic deformation during the processing of a material using the ECAP technique and to optimize the processing parameters to achieve the desired microstructure and mechanical properties while minimizing the risk of defects.

To characterize the microstructure and mechanical properties of the aluminium alloy 1050 processed by RD-ECAP, we used several techniques such as optical microscopy to observe the microstructure of the processed material and

to determine the grain size evolution as a function of the number of ECAP passes using an Olympus GX53 inverted optical microscope, micro-hardness testing in order to evaluate the distribution of micro-hardness on the longitudinal surfaces of the RD-ECAPed samples trough the pressing direction (PD) for each RD-ECAP pass (Fig. 6) using the HWDM-1 micro-hardness tester, and compression testing for the purpose of evaluating the mechanical properties of the processed samples after each RD-ECAP pass using an EZ20 testing machine by measuring the compressive yield strength and the strain hardening behaviour.

3. Results and discussions

3.1. The microstructural characterization

The optical microscope was used to examine cross sections of a material that had undergone RD-ECAP process. The examined cross sections were cut perpendicular to the axis of the extrusion (Pressing Direction). Multiple extrusions were performed depending on the numbers of RD-ECAP passes, ranging from 0 passes (the reference material) up to 10 passes. For each RD-ECAP pass, a several metallographic surface preparation steps were performed, including embedding, mechanical and electrolytic polishing, and chemical attack. The microstructure of samples was examined and the micrographs were shown in Fig. 6. A noticeable grain size refinement was observed from the first pass of the RD-ECAP process. This refinement of grain size continued to occur in all subsequent RD-ECAP passes. As the number of passes increases, the deformation accumulates, leading to further grain refinement. This is because the shear stress at the interior angle of the extrusion channel causes generation of a high density of dislocations that pile up and form new grains with a smaller size. Furthermore, at the subsequent passes, the saturation point of dislocation density is reached and the grain refinement is stopped [28, 47].

Figure 7 shows the evolution of the grain size in the initial material (0 pass) and after the RD-ECAP process at each passes (from 1 pass to 10 passes). The results were obtained through the analysis of previous micrographs (Fig. 7) using the intercept line method in the "IMAGE J" which is an image correlation software. The results obtained show a significant reduction in the grains size from the first ECAP pass. The average grain size in the initial material before ECAP was approximately 29 μm, but it dropped significantly to about 7 μm after the first RD-ECAP pass. The grain size reached its minimum value at the second RD-ECAP pass, with an average grain size of about 2 μm. From the third RD-ECAP pass, there was a slight increase in the grain size, but it remained stable until the 10th pass, with an average grain size ranging from 2.5 μm to 3.5 μm.

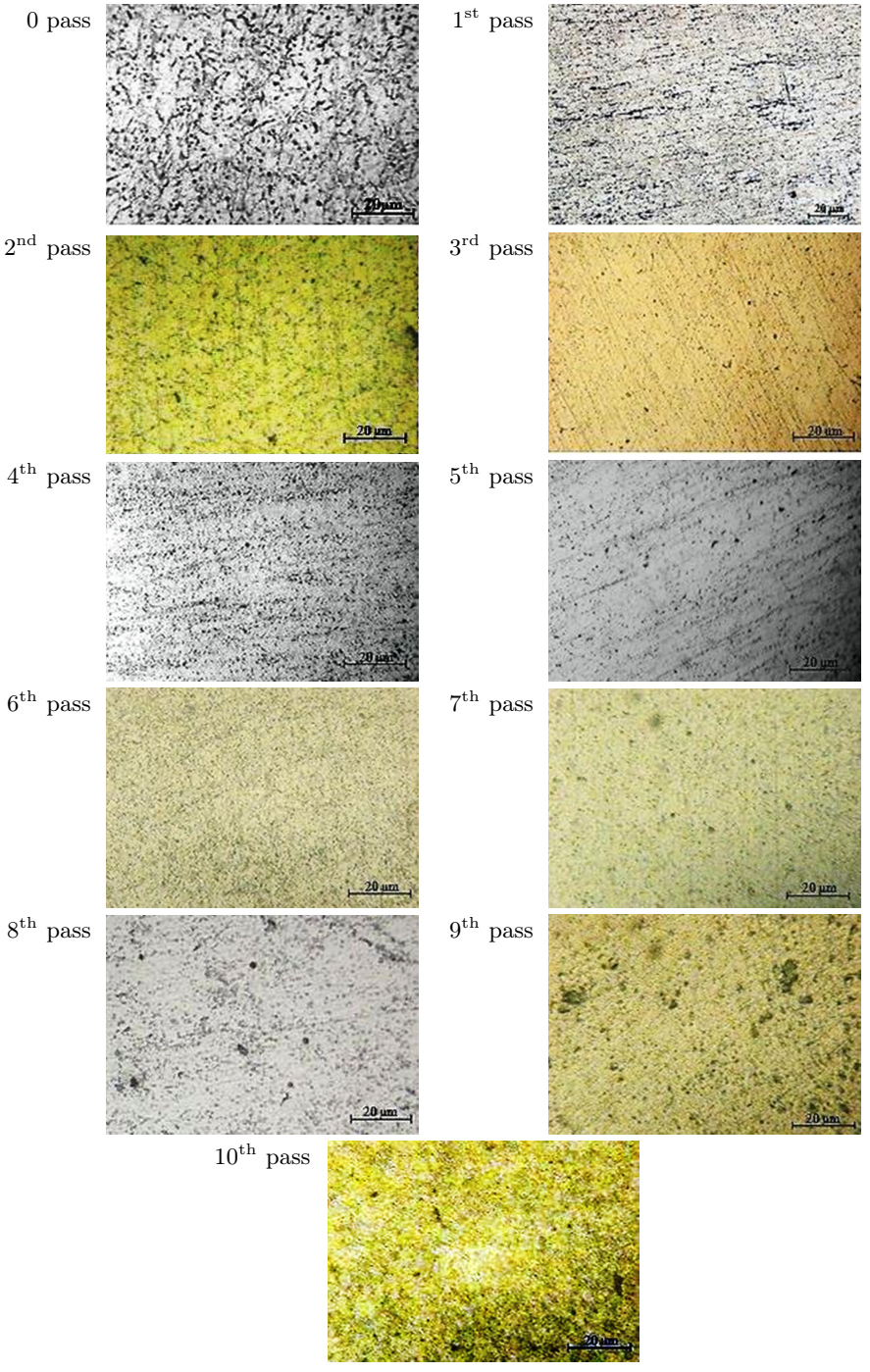

Fig. 6. Optical micrographs of the 1050 aluminium alloy processed by ECAP at different pass.

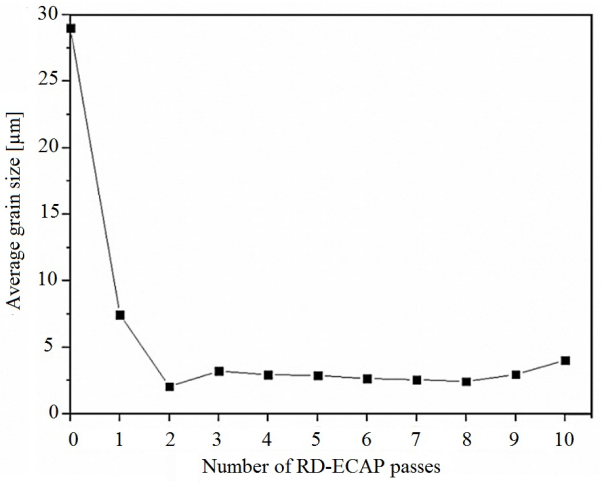

FIG. 7. Evolution of the average grain size as a function of the number of RD-ECAP passes.

The microstructural results indicate that the RD-ECAP process is an efficiency technique for producing UFG materials. The grain refinement is most significant in the early passes of the process, with the greatest reduction in the grain size occurring in the second RD-ECAP pass. Subsequent RD-ECAP passes no longer leads to a progressive grain size refinement. The results also suggest that there may be an optimal number of RD-ECAP passes to achieve a desired grain size for a given material. In this case, the grain size remained stable between the third and tenth passes, indicating that further passes may not result in significant improvements in grain size refinement.

3.2. Mechanical characterization

3.2.1. Microhardness measurements. The microhardness measurement was performed on a longitudinal plane where the measurement points belong to the surface parallel to the axis of the ECAP extrusion. Measuring microhardness on the longitudinal plane can help identify any anisotropy in the mechanical properties of the RD-ECAP processed samples. Anisotropy can arise due to the preferred grains orientation or due to the formation of strain bands in the material.

The study carried out a detailed analysis of the evolution of longitudinal microhardness as a function of the number of RD-ECAP passes over the entire surface of the sample. The microhardness measurements were taken using a refined grid pattern (Fig. 8) with a 2 mm pitch along the x-axis and a 3 mm pitch along the y-axis, where the y-axis represents the Pressing Direction (PD). This resulted in a total of 91 microhardness measurement points.

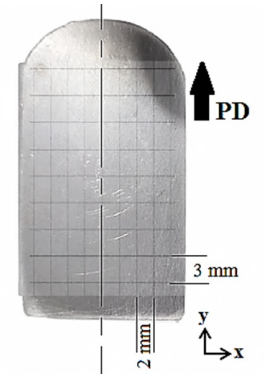

Fig. 8. The longitudinal surfaces of the RD-ECAPed sample for the micro-hardness measurement.

The results of the longitudinal microhardness measurement are presented in the form of distribution maps in Fig. 9 for each RD-ECAP pass. The maps show the distribution of microhardness values across the entire surface of the sample, and it is indicated that the microhardness values in the reference material are relatively homogeneous, ranging from 30 Hv to 35 Hv, with a maximum value of around 35 Hv. This information provides a useful reference point for understanding the changes in microhardness that occur as a result of RD-ECAP.

The microhardness of the RD-ECAP processed material increased compared to the initial material, and reached a maximum value of about 63 Hv (80% Hv of initial material) at the 4^{th} RD-ECAP cycle. This increase in microhardness is likely due to the grain size refinement that occurs during the RD-ECAP process, which leads to an increase in the number of grain boundaries and thus an increase in material strength. However, it is also noted that the distribution of the microhardness has become non-homogeneous with a significant dispersion that varies over an interval of (40 Hv, 60 Hv). This suggests that the microhardness values are no longer distributed evenly over the sample surface, but instead show a significant amount of variation. This may be due to the fact that the RD-ECAP process causes variations in the microstructure of the material that are not uniform across the sample, leading to variations in the mechanical properties such as microhardness.

The microhardness results show also that the samples of the first three RD-ECAP passes exhibit similar microhardness levels, with values varying over an interval of (36 Hv, 58 Hv). The maximum recorded value is about 58 Hv at the second RD-ECAP pass. But, there is a difference in the distribution of microhardness between these passes. In the first pass, the microhardness is highest in the area close to the external surface of the sample, in particular at the lower

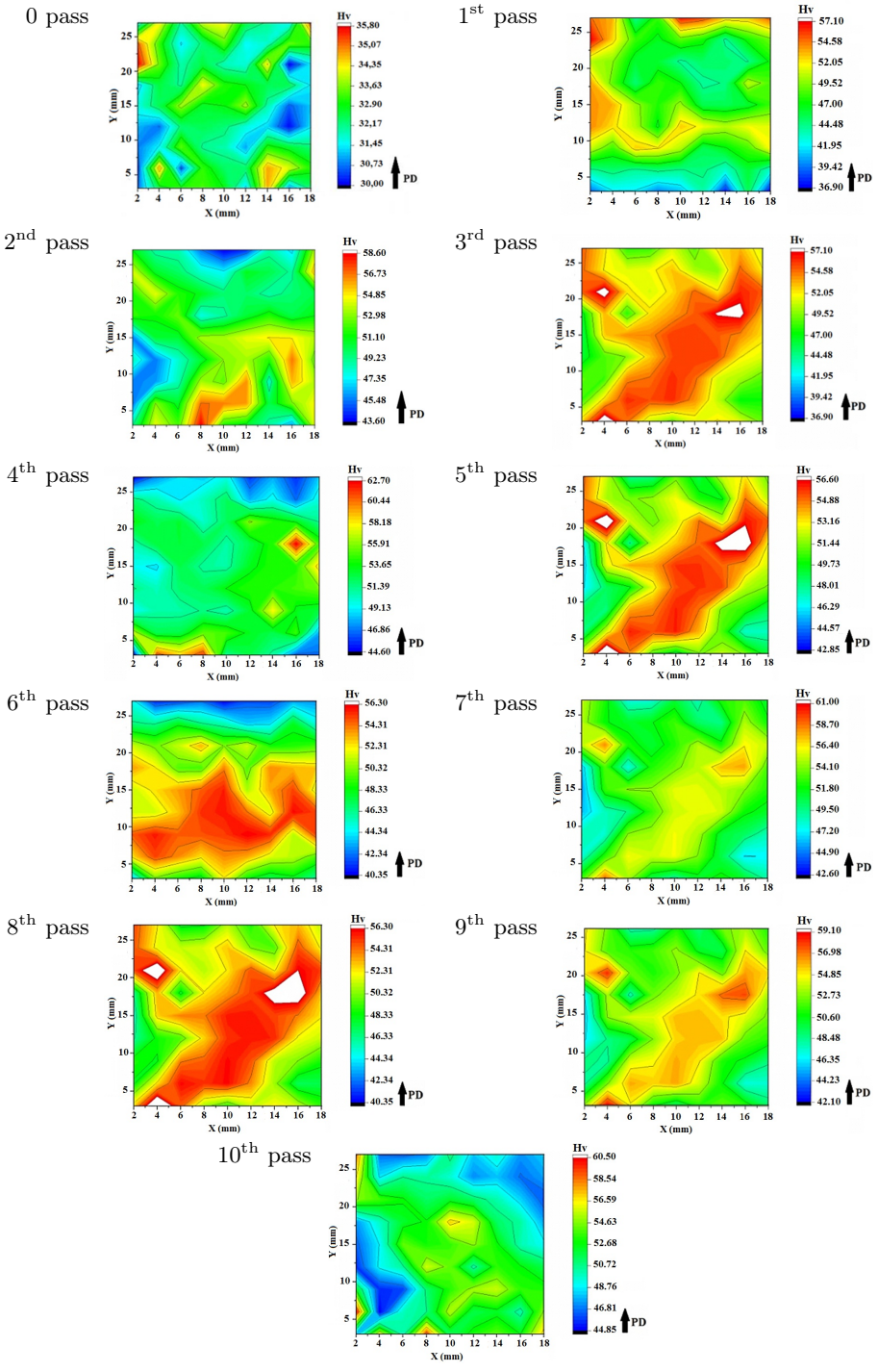

FIG. 9. Distribution maps of longitudinal microhardness as a function of the number of RD-ECAP passes.

surface (truncated) in contact with the interior angle of the ECAP channel. This is due to the significant forces applied to this area, resulting in strain hardening and thus increasing microhardness. In the second pass, the microhardness is evenly distributed over the surface of the sample, with a significant value of about 56 Hv. In the third cycle, the distribution becomes non-homogeneous, and the concentration of microhardness follows the 45° shear plane, which represents the maximum strain hardening plane resulting from the angle of the extrusion channel [14, 18]. From the 4^{th} RD-ECAP passes, the measurements of the microhardness along the longitudinal surface of samples reveal a distribution of the same level where it varies over an interval of (40 Hv, 60 Hv) and the maximum value recorded is around 63 Hv at the 4^{th} RD-ECAP passes. Interestingly, the 4^{th}, 7^{th}, and 10^{th} RD-ECAP passes all show a homogeneous distribution of microhardness along the measured surface. The 5^{th}, 6^{th}, 8^{th} and 9^{th} RD-ECAP passes show an inhomogeneous microhardness distribution similar to that of the 3^{rd} RD-ECAP pass where the concentration is at the 45° shear plane. This suggests that the distribution of microhardness varies with each RD-ECAP passes and depends on the specific deformation conditions experienced by the material during each RD-ECAP pass.

In conclusion, the microhardness distribution of UFG material produced by the RD-ECAP process depends on its microstructure. The 2^{nd} and the 4^{th} RD-ECAP pass, in particular, result in the highest grain size refinement and the most uniform distribution of microhardness with higher values. This finding confirms the Hall–Petch relationship, which states that there is an inverse relationship between hardness and grain size [1, 2]. Additionally, the application of severe plastic deformation by RD-ECAP causes the creation of shear planes at an angle of 45° to the direction of extrusion. These shear planes experience maximum strain hardening, which contributes to the local hardness of the material. When passing from one RD-ECAP pass to another, the dislocations generated during the previous pass are annihilated and rearranged due to the new shear planes having a direction opposite to the previous pass characterizing the ECAP trough the route A [25]. Thus decrease their density which explains the alternating appearance of shear planes and the homogeneity of microhardness distribution.

3.2.2. The compression test. The quasi-static compression test is being used to evaluate the mechanical properties of samples before and after the RD-ECAP process. The compression test involves applying a compressive load on the plane perpendicular to the direction of the ECAP extrusion at a displacement speed of 1mm/min. The test is carried out until the sample reaches 70% strain. The resulting stress-strain curves shown in Fig. 10 can be used to evaluate the effects of the RD-ECAP process on the yield strength, ultimate strength, and ductility of the material.

The true stress-true strain curves illustrated in Fig. 10b were generated from experimental data obtained during compression tests, initially expressed in terms of engineering stress (σ_{eng}) and engineering strain (ε_{eng}) (Fig. 10a). To achieve this representation, a conversion was necessary, employing the following formulas:

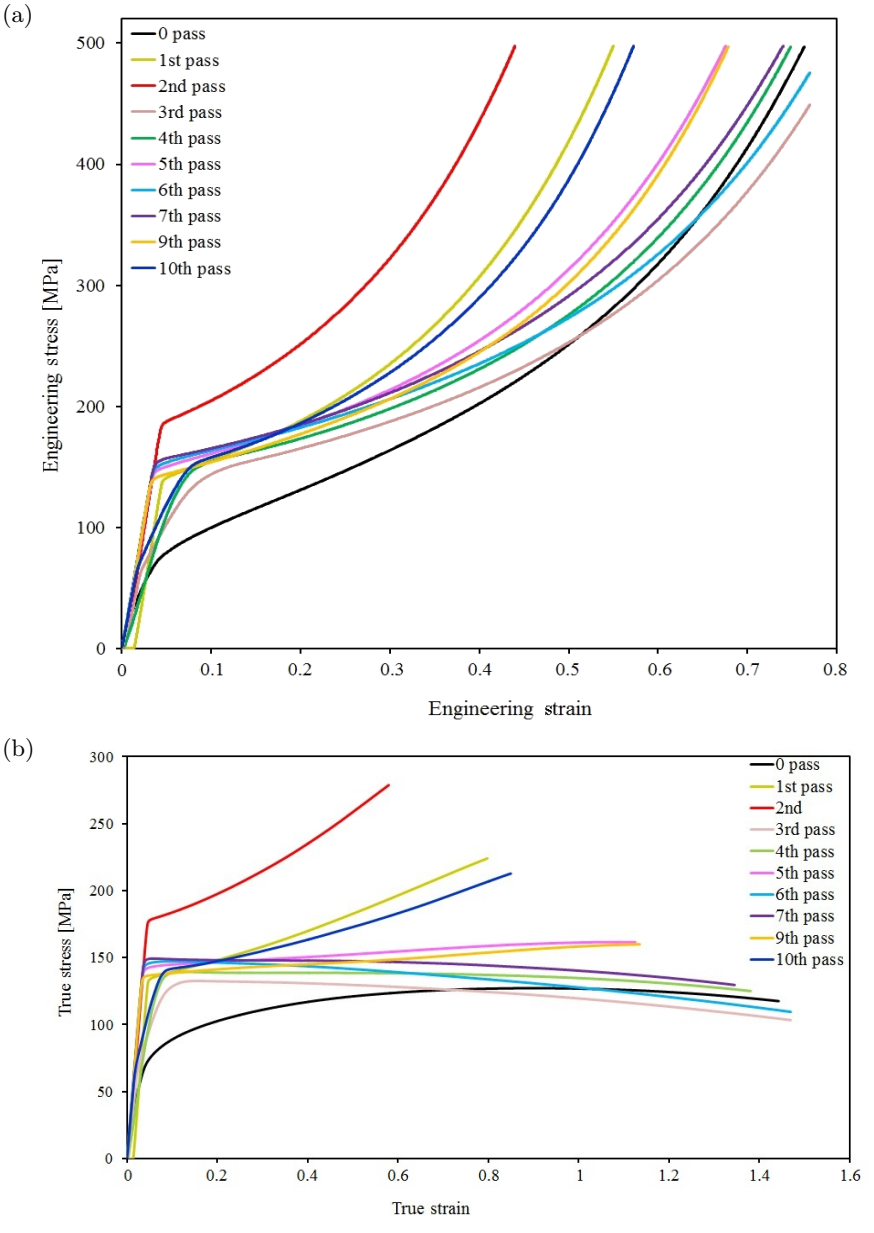

FIG. 10. Curves of the compression test of AA1050 processed by RD-ECAP at different pass: (a) engineering stress/ engineering strain (b) true stress/ true strain.

- True strain $= -\ln(1 - \varepsilon_{\text{eng}})$.
- True stress $= \sigma_{\text{eng}} \times (1 - \varepsilon_{\text{eng}})$.

The stress-strain curves obtained from the different studied cases exhibit a similar shape, with two distinct regions: a linear elastic region, followed by a plastic region with an increasing linear aspect that indicates strain hardening of the material. The results of the quasi-static compression tests are presented in Fig. 11 which shows the compressive yield strength (Re/c) as a function of the number of RD-ECAP pass, where Re/c is the stress at which the material starts to deform plastically.

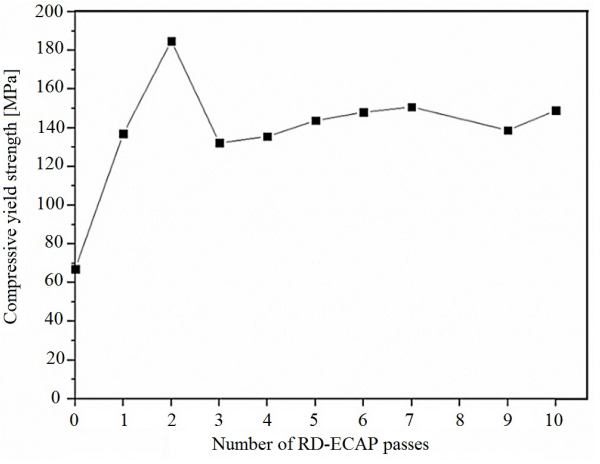

Fig. 11. Compressive yield strength (Re/c) as a function of the number of RD-ECAP passes.

The Re/c of the material increased from the 1st RD-ECAP pass, which reached a maximum value of 184.89 MPa at the 2nd pass, this increase was significant and represents 2.75 times that of the initial material before RD-ECAP. Despite, a slight decrease in Re/c was noticed at the 3rd RD-ECAP passes and its return to rising from the 4th RD-ECAP passes.

The grain size refinement is attributed to the formation of barriers in the form of grain boundaries, which act as obstacles to dislocation movement and lead to their accumulation. Therefore, the kinetics of the dislocations is controlled by the barriers formed during the process of severe plastic deformation, which in turn affects the grain size refinement through ECAP and the material strength [10, 48].

In fact, the compressive yield strength increased from the 1st RD-ECAP pass was due to a grain size refinement, and the maximum improvement was in the 2nd RD-ECAP pass, which shows the best grain size refinement. Indeed, the grain size at the 3rd RD-ECAP passes decrease slightly, which explains the decrease of Re/c. Moreover, the slight rise in the compressive yield strength from the 4th

pass was due to the recovery phenomena introduced into the microstructure of material, which regains its strength after the initial decrease at the 3rd pass due to the thermal energy converted from the strong accumulation of dislocations due to severe plastic deformation applied at the subsequent passes [10, 48].

Overall, RD-ECAP which is a severe plastic deformation process used to refine the grain size and increase the density of grain boundaries and obstacles to dislocation movement. Moreover, the compressive yield strength of the material increases with the number of RD-ECAP passes, corresponding to the refinement of grain size, thus increasing the number of obstacles to dislocation movement. The highest value of the compressive yield strength is observed in the sample after the second pass of RD-ECAP, which has the smallest grain size, which correlate with the Hall–Petch relation [1, 2].

In addition, another phenomenon that occurs during the RD-ECAP process is recrystallization/restoration mechanism. This phenomenon occurs when the dislocation density reaches a saturation threshold and the stacking energy is partly transformed into thermal energy, leading to the initiation of restoration by the annihilation of dislocations and dynamic recrystallization of the microstructure through the creation of new grains [10, 48]. As a result of this phenomenon, the grain size increases and the compressive yield strength decreases after the 2nd RD-ECAP pass. Indeed, the increase in grain size reduces the density of grain boundaries and obstacles to dislocation movement, which leads to a reduction in strength.

In conclusion, the RD-ECAP process had a significant effect on the compressive yield strength of the material, with both increases and decreases observed as a function of the number of passes. However, The peak value of 184.89 MPa after the 2nd ECAP pass represents a further improvement in the compressive yield strength, which means that the RD-ECAP process was effective in strengthening the material through grain size refinement, but the subsequent decrease in the compressive yield strength after the 2nd pass proves that there is a limit to the amount of improvement that can be achieved by the RD-ECAP process.

3.2.3. The strain hardening behaviour. The strain hardening coefficient provides an indication of how a material behaves during plastic deformation. However, if a material has a high strain hardening coefficient, it means that it will exhibit significant strengthening as it is deformed. On the other hand, materials with a low strain hardening coefficient may exhibit less strengthening during deformation and may be more prone to localized deformation or necking, which can reduce their formability. Therefore, materials with a high strain hardening coefficient are generally preferred for forming applications where improved formability and mechanical properties are desired. However, it is important to note that the value of the strain hardening coefficient may vary with the plastic strain and temper-

ature of the material during the RD-ECAP process. Therefore, it is necessary to determine the value of strain hardening coefficient at each stage of the RD-ECAP process to fully understand the strain hardening behaviour of the material.

In general, Hollomon's law relates the stress-strain behaviour of a metal to the metal's microstructure and deformation properties. The strain hardening coefficient is one of the parameters used in Hollomon's law to describe the extent to which a metal's strength increases with plastic deformation. To calculate the strain hardening coefficient, the equation used typically involves the relationship between the flow stress (σ) and the strain rate (ε) during plastic deformation. This equation is often expressed as: $\sigma = k\varepsilon_p^n$ [49]; where k is a material constant and n is the strain hardening coefficient. The value of n depends on the material being deformed and the conditions of the deformation process.

The evolution of the strain hardening coefficient as a function of the number of RD-ECAP passes (shown in Fig. 12) will depend on various factors, such as the starting microstructure of the material, the strain rate, the temperature, and the total deformation applied. Indeed, as the number of RD-ECAP passes increases, the material's microstructure will change, leading to changes in the material's properties and the value of the strain hardening coefficient.

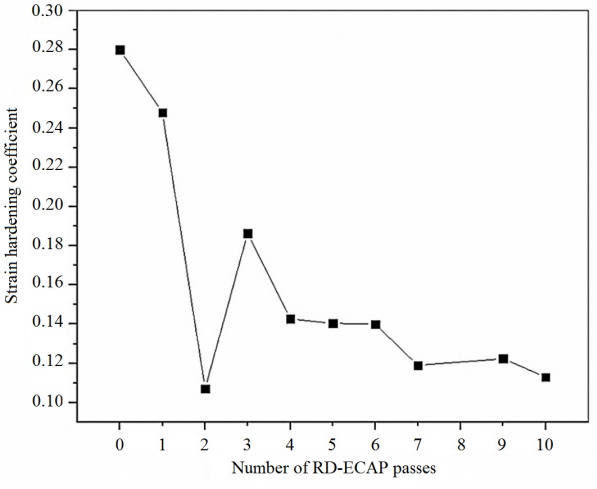

Fig. 12. Evolution of the strain hardening coefficient of each pass of the RD-ECAP process.

The results observed of the evolution of the strain hardening coefficient of the material during the RD-ECAP process show that there is a decrease in "n" from the first RD-ECAP pass despite a refinement of the grain size and an increase of the compressive yield strength and presents a minimum value in the second pass which has the best grain size refinement and the highest microhardness and compressive yield strength. This suggests that the material has almost lost its strain hardening capacity. This phenomenon is common in severely deformed

materials, where the high strain causes a change in the microstructure, such as the creation of defects or the fragmentation of grains, leading to a decrease in the strain hardening exponent [49].

After 2 RD-ECAP passes the value of n decreases drastically. This decrease in the n coefficient could be attributed to the microstructure heterogeneity, which leads to a reduction in the material's ability to increase its strength during plastic deformation, resulting in a decrease in the strain hardening exponent. Furthermore, there is a considerable reduction in the grain size after two passes, which means that there is less mobility for dislocations. The dislocations present defects in the crystal lattice, which allow plastic deformation to occur. Therefore, a reduction in dislocation movement may lead to a decrease in the strain hardening exponent [49].

Moreover, for the 3rd RD-ECAP pass, there is a small increase in the coefficient n, followed by a further decrease for subsequent passes up to 10 passes. This fluctuation in the n coefficient could be attributed to a new change in the microstructure nature. As the material undergoes more passes of severe plastic deformation, there could be a continuous change in the microstructure, which can affect the material's strain hardening behavior. Indeed, it is worth noting that the strength and hardness of the material do not only depend on strain hardening behaviour. Other factors such as the nature and distribution of impurities, microstructural defects, and residual stresses can also influence the material's mechanical properties. Therefore, a reduction in the strain hardening coefficient does not necessarily result in a corresponding reduction in strength or hardness.

Nevertheless, during the RD-ECAP process, the material undergoes severe plastic deformation, resulting in a significant amount of strain hardening and grain refinement. However, as the number of RD-ECAP passes increases, the strain hardening coefficient may decrease, even though the grain size refinement and compressive yield strength increase. There are several factors that may contribute to the observed decrease in the strain hardening coefficient during the RD-ECAP process. Firstly, as the material becomes more strain hardened, its ability to deform decreases, leading to a decrease in the strain hardening coefficient. Additionally, the increase in the compressive yield strength could be due to the material's increased strength and not necessarily due to its ability to harden during deformation. Moreover, dynamic recovery/recrystallization and other microstructural changes may occur during deformation, leading to changes in the strain hardening behaviour.

4. Applications

The AA1050 aluminum alloy, distinguished by its commercial purity, high electrical conductivity, and remarkable formability, also exhibits ductility that

limits its range of applications and lifespan. The Equal Channel Angular Pressing (ECAP) technique will impart elevated mechanical characteristics to aluminium AA1050, approaching those of widely used alloys such as the 2000 series, while preserving its purity. Well-known applications of the AA1050 alloy could thus be retained, with improvements in mechanical strength and durability achieved through ECAP. This would make it applicable in areas such as electrical conductors, connectors, and various components in the electrical and electronics industry. Moreover, in sectors where thermal conductivity is crucial, such as in heat exchangers, ECAP processing of aluminium 1050 could enhance its strength without compromising its thermal properties, resulting in more durable heat exchanger fins. The use of this alloy in applications like reflective surfaces, architectural elements, laboratory equipment, consumer electronics housings, as well as automotive trim and decorative elements, could also benefit from the ECAP treatment, providing enhanced resistance for increased durability while preserving the inherent characteristics of lightweight and corrosion resistance specific to this alloy.

5. Conclusion

In summary, ultrafine-grained AA1050 Aluminium Alloy was achieved through the 10-pass RD-ECAP process at room temperature. The evolution of the microstructure and mechanical properties of the samples, both before and after the RD-ECAP process, was systematically investigated at each pass. The results highlighted the relationship between grain refinement and mechanical characteristics. Specifically, microhardness and compressive yield strength exhibited enhancement with decreasing grain size, consistent with the Hall–Petch relationship. The findings indicated that the significant improvement in both microstructure and mechanical behaviour of the RD-ECAPed AA1050 aluminium alloy was attained at the second pass, characterized by an average grain size of about 2 μm, a compressive yield strength (Re/c) of 184 MPa, and a microhardness (Hv) of 63 with a homogeneous distribution.

References

1. E.O. Hall, *The deformation and ageing of mild steel*, Proceedings of the Physical Society-Section B, **64**, 9, 747–753, 1951, doi:10.1088/0370-1301/64/9/303.

2. N.J. Petch, *The cleavage strength of polycrystals*, Journal of the Iron and Steel Institute, **174**, 25–28, 1953.

3. T.G. Langdon, *Twenty-five years of ultrafine-grained materials: achieving exceptional properties through grain refinement*, Acta Materialia, **61**, 19, 7035–7059, 2013, doi: 10.1016/j.actamat.2013.08.018.

4. G. FARAJI, H.S. KIM, H.T. KASHI, *Severe Plastic Deformation: Methods, Processing and Properties*, Elsevier, 2018, doi: 10.1016/C2016-0-05256-7.

5. M. SHEIK HASSAN, S. SHARMA, B. KUMAR, *A review of severe plastic deformation*, International Refereed Journal of Engineering and Science (IRJES), **6**, 7, 66–85, 2017.

6. R.Z. VALIEV, Y. ESTRIN, Z. HORITA, T.G. LANGDON, M.J. ZECHETBAUER, Y.T. ZHU, *Producing bulk ultrafine-grained materials by severe plastic deformation*, JOM (TMS) (Minerals, Metals & Materials Society), **58**, 4, 33–39, 2006, doi: 10.1007/s11837-006-0213-7.

7. R. VALIEV, *Nanostructuring of metals by severe plastic deformation for advanced properties*, Nature Materials, **3**, 8, 511–516, 2004, doi: 10.1038/nmat1180.

8. C. WANG, F. LI, B. CHEN, Z. YUAN, H. LU, *Severe plastic deformation techniques for bulk ultrafine-grained materials*, Rare Metal Materials and Engineering, **41**, 6, 941–946, 2012, doi: 10.1016/S1875-5372(12)60049-6.

9. Y. SAITO, H. UTSUNOMIYA, N. TSUJI, T. SAKAI, *Novel ultra-high straining process for bulk materials-Development of the accumulative roll bonding (ARB) process*, Acta Materialia, **47**, 579–583, 1999, doi: 10.1016/S1359-6454(98)00365-6.

10. A. HALIMI, A. BOUDIAF, L. HEMMOUCHE, A. MEDJAHED, D.E. TRIA, A. HENNICHE, M.E.A. DJEGHLAL, T. BAUDIN, *Quasi-static and dynamic characterization of ultrafine-grained 2017A-T4 aluminium alloy processed by accumulative roll bonding*, Archives of Mechanics, **73**, 4, 339–363, 2021, doi: 10.24423/aom.3795.

11. P.S. SAHOO, M.M. MAHAPATRA, P.R. VUNDAVILLI, C. PANDEY, *Effects of working temperature on microstructure and hardness of Ti-6Al-4V alloy subjected to asymmetrical rolling*, Journal of Materials Engineering and Performance, 2023, doi: 10.1007/s11665-023-08076-0.

12. A.P. ZHILYAEV, T.G. LANGDON, *Using high-pressure torsion for metal processing: Fundamentals and applications*, Progress in Materials Science, **53**, 893–979, 2008, doi: 10.1016/j.pmatsci.2008.03.002.

13. A. ZHILYAEV, G. NURISLAMOVA, B.-K. KIM, M. BARÓ, J. SZPUNAR, T. LANGDON, *Experimental parameters influencing grain refinement and microstructural evolution during high-pressure torsion*, Acta Materialia, **51**, 3, 753–765, 2003, doi: 10.1016/S1359-6454(02)00466-4.

14. M. FURUKAWA, Z. HORITA, M. NEMOTO, T.G. LANGDON, *Review: processing of metals by equal-channel angular pressing*, Journal of Materials Science, **36**, 2835–2843, 2001, doi: 10.1023/A:1017932417043.

15. R.Z. VALIEV, T.G. LANGDON, *Principles of equal-channel angular pressing as a processing tool for grain refinement*, Progress in Materials Science, **51**, 881–981, 2006, doi: 10.1016/j.pmatsci.2006.02.003.

16. V.M. SEGAL, *Equal channel angular extrusion: from macromechanics to structure formation*, Materials Science and Engineering A, **271**, 322–333, 1999, doi: 10.1016/S0921-5093(99)00248-8.

17. E. EL-DANAF, M. KAWASAKI, M. EL-RAYES, M. BAIG, J.A. MOHAMMED, T.G. LANGDON, *Mechanical properties and microstructure evolution in an aluminium 6082 alloy processed by high-pressure torsion*, Journal of Materials Science, **49**, 19, 6597–6607, 2014, doi: 10.1007/s10853-014-8266-4.

18. P. Vishnu, R. Raj Mohan, E. Krishna Sangeethaa, S. Raghuraman, R. Venkatraman, *A review on processing of aluminium and its alloys through Equal Channel Angular Pressing die*, Materials Today: Proceedings, **21**, 212–222, 2019, doi: 10.1016/j.matpr.2019.04.223.

19. L. Cui, S. Shao, H. Wang, G. Zhang, Z. Zhao, C. Zhao, *Review: recent advances in the equal channel angular pressing of metallic materials*, Processes, **10**, 2181, 2022, doi: 10.3390/pr10112181.

20. P.S. Sahoo, A. Meher, M.M Mahapatra, R.V. Pandu, *Analysis of mechanical and microstructural characteristics of plunger-assisted ECAP strengthened Ti-6Al-4V alloy sheets*, Archives of Civil and Mechanical Engineering, **23**, 194, 2023, doi: 10.1007/s43452-023-00742-3.

21. Z. Horita, M. Furukawa, M. Nemoto, T.G. Langdon, *Development of fine grained structures using severe plastic deformation*, Materials Science and Technology, **16**, 11–12, 1239–1245, 2000, doi: 10.1179/026708300101507091.

22. H. Sato, S. El Hadad, O. Sitdikov, Y. Watanabe, *Effects of processing routes on wear property of Al-Al$_3$Ti alloys severely deformed by ECAP*, Materials Science Forum, **584-586**, 971–976, 2008, doi: 10.4028/www.scientific.net/MSF.584-586.971.

23. K. Oh-Ishi, Z. Horita, M. Furukawa, M. Nemoto, T.G. Langdon, *Optimizing the rotation conditions for grain refinement in equal-channel angular pressing*, Metallurgical and Materials Transactions A, **29**, 7, 2011–2013, 1998, doi: 10.1007/s11661-998-0027-z.

24. S. Akramov, I. Kim, M.G. Lee, B.H. Park, *Sheet formability of AA 1050 Al alloy sheet by equal channel angular pressing of route C type*, Solid State Phenomena, **116-117**, 324–327, 2006, doi: 10.4028/www.scientific.net/SSP.116-117.324.

25. M.C.V. Vega, R.E. Bolmaro, M. Ferrante, V.L. Sordi, A.M. Kliauga, *The influence of deformation path on strain characteristics of AA1050 aluminium processed by equal-channel angular pressing followed by rolling*, Materials Science and Engineering: A, **646**, 154–162, 2015, doi: 10.1016/j.msea.2015.07.083.

26. S.R. Kumar, K. Gudimetla, P. Venkatachalam, B. Ravisankar, K. Jayasankar, *Microstructural and mechanical properties of Al 7075 alloy processed by equal channel angular pressing*, Materials Science and Engineering: A, **533**, 50–54, 2012, doi: 10.1016/j.msea.2011.11.031.

27. P. Venkatachalam, S.R. Kumar, B. Ravisankar, V.T. Paul, M. Vijayalakshmi, *Effect of processing routes on microstructure and mechanical properties of 2014 Al alloy processed by equal channel angular pressing*, Transactions of Nonferrous Metals Society of China, **20**, 10, 1822–1828, 2010, doi: 10.1016/S1003-6326(09)60380-0.

28. T. Kovaříka, J. Zrnikb, M. Cieslard, *Grain refinement in aluminium alloy AlMgSi1 during ECAP at room temperature*, Health and Environmental Research Online (HERO), **19**, 121–126, 2009.

29. J. Mao, S. Kang, J. Park, *Grain refinement, thermal stability and tensile properties of 2024 aluminium alloy after equal-channel angular pressing*, Journal of Materials Processing Technology, **159**, 3, 314–320, 2005, doi: 10.1016/j.jmatprotec.2004.05.020.

30. G. Prashanth, *Ultra-grain refinement and optimization of aluminium material properties using equal channel angular pressing (ECAP) in deform software*, International Journal of Scientific Research and Review, **8**, 6, 145, 2019.

31. M. HOWEYZE, H. ARABI, A. EIVANI, H. JAFARIAN, *Strengthening of AA5052 aluminium alloy by equal channel angular pressing followed by softening at room temperature*, Materials Science and Engineering: A, **720**, 160–168, 2018, doi: 10.1016/j.msea.2018.02.054.

32. M. GOODARZY, H. ARABI, M. BOUTORABI, S. SEYEDEIN, S.H. NAJAFABADI, *The effects of room temperature ECAP and subsequent aging on mechanical properties of 2024 al alloy*, Journal of alloys and compounds, **585**, 753–759, 2014, doi: 10.1016/j.jallcom.2013.09.202.

33. A. YAMASHITA, D. YAMAGUCHI, Z. HORITA, T.G. LANGDON, *Influence of pressing temperature on microstructural development in equal-channel angular pressing*, Materials Science and Engineering: A, **287**, 1, 100–106, 2000, doi: 10.1016/S0921-5093(00)00836-4.

34. I. MAZURINA, T. SAKAI, H. MIURA, O. SITDIKOV, R. KAIBYSHEV, *Effect of deformation temperature on microstructure evolution in aluminium alloy 2219 during hot ECAP*, Materials Science and Engineering: A, **486**, 1-2, 662–671, 2008, doi: 10.1016/j.msea.2007.09.070.

35. L. SU, G. DENG, V. LUZIN, H. WANG, Z. WANG, H. YU, H. LI, A.K. TIEU, *Effect of cryogenic temperature equal channel angular pressing on microstructure, bulk texture and tensile properties of AA1050*, Materials Science and Engineering A, **780**, 139190, 2020, doi: 10.1016/j.msea.2020.139190.

36. M. SHAERI, M. SHAERI, M. EBRAHIMI, M. SALEHI, S. SEYYEDEIN, *Effect of ECAP temperature on microstructure and mechanical properties of Al–Zn–Mg–Cu alloy*, Progress in Natural Science: Materials International, **26**, 2, 182–191, 2016, doi: 10.1016/j.pnsc.2016.03.003.

37. P. KOPROWSKI, R. BOGUCKI, M. BIEDA, J. KAWAŁKO, K. SZTWIERTNIA, *Thermal stability of AA1050 aluminium alloy after equal channel angular pressing*, Archives of Metallurgy and Materials, **62**, 2, 777–786, 2017, doi: 10.1515/amm-2017-0116.

38. S.L. SEMIATIN, P.B. BERBON, T.G. LANGDON, *Deformation heating and its effect on grain size evolution during equal channel angular extrusion*, Scripta Materialia, **44**, 135–140, 2001, doi: 10.1016/S1359-6462(00)00565-0.

39. T. CAMALET, A. RUSINEK, R. BERNIER, M. KARON, R. MASSION, G. VOYIADJIS, M. ADAMIAK, *Effect of severe plastic deformation by 120 deg ECAP or shock impact on 6061 aluminium alloy at high strain rates*, Journal of Engineering Materials and Technology, **140**, 4, 2018, doi: 10.1115/1.4039690.

40. P. B. BERBON, M. FURUKAWA, Z. HORITA, M. NEMOTO, T.G. LANGDON, *Influence of pressing speed on microstructural development in equal-channel angular pressing*, Metallurgical and Materials Transactions A, **30A**, 1989–1997, 1999, doi: 10.1007/s11661-999-0009-9.

41. O. ABIOYE, P. ATANDA, G. OSINKOLU, A. ABIOYE, I. OLUMOR, O. ODUNLAMI, S. AFOLALU, *Influence of equal channel angular extrusion on the tensile behaviour of aluminium 6063 alloy*, Procedia Manufacturing, **35**, 1337–1343, 2019, doi: 10.1016/j.promfg.2019.05.020.

42. T.Q. PHAN, L.E. LEVINE, I-F. LEE, R. XU , J.Z. TISCHLER, Y. HUANG, T.G. LANGDON, M.E. KASSNER, *Synchrotron X-ray microbeam diffraction measurements of full elastic long range internal strain and stress tensors in commercial-purity aluminium processed by multiple passes of equal-channel angular pressing*, Acta Materialia, **112**, 231–241, 2016, doi: 10.1016/j.actamat.2016.04.035.

43. F. Djavanroodi, B. Omranpour, M. Ebrahimi, M. Sedighi, *Designing of ECAP parameters based on strain distribution uniformity*, Progress in Natural Science: Materials International, **22**, 5, 452–460, 2012, doi: 10.1016/j.pnsc.2012.08.001.

44. H.S. Kim, M.H. Seo, S.I. Hong, *On the die corner gap formation in equal channel angular pressing*, Materials Science and Engineering: A, **291**, 1-2, 86–90, 2000, doi: 10.1016/S0921-5093(00)00970-9.

45. Y. Nishida, H. Arima, J.C. Kim, T. Ando, *Development of the ECAP with a rotary die and its application to AC4C aluminum alloy*, Journal of Japan Institute of Light Metals, **50-12**, 655–659, 2000, doi: 10.2464/jilm.50.655.

46. A. Watazua, I. Shigematsub, M. Hakamadac, K. Suzukid, X.S. Huange, N. Saito, *Rotary-die equal channel angular pressing method for Light metals*, Materials Science Forum, **638-642**, 1614–1617, 2010, doi: 10.4028/www.scientific.net/MSF.638-642.1614.

47. R. Kaibyshev, S. Malopheyev, V. Kulitskiy, M. Gazizov, *The role of deformation banding in grain refinement under ECAP*, Materials Science Forum, **783**, 2641–2646, 2014, doi: 10.4028/www.scientific.net/MSF.783-786.2641.

48. A. Kobaissy, G. Ayoub, W. Nasim, J. Malik, I. Karaman, M. Shehadeh, *Modeling of the ECAP induced strain hardening behavior in FCC metals*, Metallurgical and Materials Transactions A, **51A**, 5453–5474, 2020, doi: 10.1007/s11661-020-05971-2.

49. J.A. Muñoz Bolaños, O.F. Higuera Cobos, J.M. Cabrera Marrero, *Strain hardening behavior of ARMCO iron processed by ECAP*, Materials Science and Engineering, **63**, 012143, 2014, doi: 10.1088/1757-899X/63/1/012143.

50. W.J. Kim, C.S. Chung, D.S. Ma, S.I. Hong, H.K. Kim, *Optimization of strength and ductility of 2024 Al by equal channel angular pressing (ECAP) and post-ECAP aging*, Scripta Materialia, **49**, 333–338, 2003, doi: 10.1016/S1359-6462(03)00260-4.

Received July 6, 2023; revised version December 24, 2023.
Published online January 18, 2024.